Axial and radial patterns of a bidispersed suspension in a fully filled horizontal rotating cylinder

John C. Nasaba and Anugrah Singh*
Department of Chemical Engineering, Indian Institute of Technology Guwahati, 781039-Guwahati, Assam, India

(Received 29 June 2018; published 6 November 2018)

We report on the pattern formation in a horizontal rotating cylinder fully filled with bidispersed suspension composed of non-Brownian settling and floating particles. The effect of particle mixing of different buoyancy and shape on the axial and radial pattern formation was investigated using flow visualization and particle image velocimetry techniques. The experimental investigations involved two cases divided according to the shape of the particles making up the suspension. In the first case, both the floating and settling particles were spherical in shape while the second one was composed of buoyant spherical and settling cylindrical particles. A detailed analysis of the difference between the monodispersed and bidispersed suspension for various rotational speeds is provided. The radial and axial patterns for the bidispersed suspension was found to strongly depend on the rotation rate. The behavior at low rotation was similar to that of monodispersed systems, but at higher speeds, hybrid patterns emerged that were driven by the complementary influence of the two kinds of particles. The patterns observed were seen to be primarily influenced by the particle-particle hydrodynamic interaction. The nonspherical nature of the cylindrical particles produces radial and axial patterns that are distinctly different from the spherical particles.

DOI: 10.1103/PhysRevE.98.053102

I. INTRODUCTION

Throughout nature and in a broad range of technological applications, the flow of solid particles suspended in a continuous liquid phase is common [1,2]. This includes, among others, flow of mud, glass fibers in polymer solutions, sedimentation, as well as particle transport. Since many industrial processes are dominated by these flows, their study has become a vibrant area of research [3]. In several studies the horizontal rotating drum is taken as a pivotal experimental configuration that has assisted in the study of an array of phenomena stretching beyond scientific research to profound industrial applications. These include the pharmaceutical industry and wood debarking in paper making industry. A fact worth noticing is that the two-phase particulate flows comprise a complex interlink of particle and fluid properties, each having a contribution to the ultimate behavior of the system. The dominant interactions characterizing particles dispersed in a liquid phase are the particle-particle interactions and the particle-fluid interactions [4].

The shape of the particles in a suspension is a parameter that has the ability to influence the behavior of a suspension. A substantial amount of work has been done to understand the hydrodynamics of nonspherical particles. These particles, when subjected to simple shear, rotate about the vorticity axis and their rotation absorbs part of the bulk strain experienced by the suspension [5]. Brenner [6], by determination of the Einstein coefficient, showed that the corresponding value of the free to rotate particles was lower than that for the nonrotating ones. Particles in suspensions display a wide variety of surprising characters, such as sedimentation, segregation, etc. The flow behavior of suspension shows a complex dependence on its physical properties and the processes occurring at the scale of the suspended particles. The interest in studying the pattern formation in rotating suspension increased since the experimental work of Tirumkudulu *et al.* [7]. They observed that the neutrally buoyant suspension in a partially filled horizontal rotating Couette geometry segregate into alternating regions of high and low particle concentration along the axis. The high concentration regions were situated underneath crests and the low concentration regions below the troughs of the wavy interface. No segregation was observed when the Couette was completely filled, suggesting that a free surface is necessary for this phenomenon to occur. The observation of particle segregation patterns by Lipson [8] during a study on crystallization of ammonium chloride crystals suspended in a supersaturated solution was unexpected since there was no free surface. It was also reported that this phenomenon occurred for positively buoyant particles (air bubbles) [9]. These findings then became a driving force behind further research to fully comprehend the observed phenomena. Matson *et al.* [10] reported pattern formation in a rotating suspension of non-Brownian settling particles. They conducted experiments in horizontal rotating cylinder for various rotation rates and different solvent viscosity and observed nine different steady states by their unique flow patterns and particle distributions. These studies have been followed up by several experimental and theoretical investigations to understand the factors that influence the pattern formation. The most important factors are particle volume fraction (ϕ), particle shape, interactions between particles, the spatial arrangement of particles, and the nature of the bulk flow field [5]. The primary active forces on particles in a rotating suspension are the viscous drag, gravitational and centrifugal forces [11–13]. When a heavy particle is

*anugrah@iitg.ernet.in

suspended in a rotating fluid, the net force is such that it spirals toward the cylinder wall. However, for rotating suspension of settling particles the dynamics are different for a collection of particles due to complex hydrodynamic interactions [10]. When settling particles are suspended at low volume fraction in a rotating cylinder, three main scenarios are possible depending on the rotation rate [14,15]. For rotation rates below the critical value Ω_L, the buoyancy force dominates and the particles accumulate adjacent to the rising wall of the rotating cylinder. For intermediate values ($\Omega_L < \Omega < \Omega_H$), axial segregation takes place and periodically spaced bands of high particle concentration having a wavelength λ are observed. When the rotation rates are large ($\Omega > \Omega_H$), the centrifugal force dominates and the particles form a uniform thin layer adjacent to the surface of the cylinder.

The dependence of pattern formation on the cylinder length L and the particle parameters i.e., size, shape, and density was carried out by Seiden *et al.* [16]. They studied several monodispersed suspensions composed of nylon, polystyrene, plexiglass particles, etc., suspended in a rotating fluid. Seiden *et al.* [17] observed a sawtoothlike pattern along the cylinder length. No substantial dependency on the characteristics of the particles was seen for the speed ranges they explored. The bands formed either adjacent to or half a wavelength away from the end wall, and hence for each cylinder length, there were two potential band configurations. They also stated that in a number of cases, the bands oscillate periodically between two interleaving patterns and put forward the argument that banding is caused by the excitation of inertial standing waves in the rotating fluid. They acknowledged what Lee and Ladd [18] put forward, suggesting that the mechanism involving the balance between gravitational, viscous, and centrifugal forces cause particles to segregate into axial bands with separation (Λ) independent of rotational rate, the viscosity of the fluid, and the geometry of the particles. For crystals and bubbles, the bands were very narrow and well defined. When bubbles were present together with particles, bubble bands interleaved with the particle bands. The band spacing (Λ) were measured as a function of the cylinder length L. Bands were seen to be at intervals of Λ and not $\Lambda/2$.

Seiden *et al.* [16] performed experiments in which both the motion of a single particle as well as collection of particles was analyzed. For the case of a single particle, an off-center neutral point on the horizontal axis was found where it could remain in equilibrium between the drag and gravitational forces, or at which stable circulation occurred. Lee and Ladd [18] showed that this equilibrium point is unstable in the low Reynolds number regime though particles would remain there for long periods. In many cases, when the bands formed, the particles moved within a fairly well-defined torus around the neutral point. During oscillations a new band results from the meeting of adjacent bands. Axial banding of larger particles (Re $>>$ 1) was also reported by Breu and Rehberg [19], Lipson [8] and Lipson and Seiden [9] and the average separation between two consecutive bands was found to lie between $3.5R$ and $4R$. Breu and Rehberg [19] conducted an experimental study to explain the banding of much larger particles in rotating fluids of negligible viscosity; with Reynolds number of the order of 100–300. From the work of Lipson [8] and Lipson and Seiden [9], it is ascertained that banding is independent of rotational rate and occurs for a wide range of particle types and sizes. Matson *et al.* [3,10] carried out detailed experimental investigations on the various states observed with variation of the rotation and the fluid viscosity. They reported nine different states, ranging from granular bed state (GB) found at low rotation to the centrifugal limit (CL) state, which characterizes the high rotation rates. Matson *et al.* [15] broadened the investigation to include the effects of the particle size, concentration, and the cylinder radius. Their experiments showed that varying the particle size has an effect mainly on the transition between states but not on the character and number of observed states. Their results also indicate that the dominant influence of the particle concentration is an increase of gravitational driving force, instead of effective viscosity of the suspension. When varying the cylinder radius all the states observed by Matson *et al.* [3] were recovered apart from the homogeneous region (HR) state. Kalyankar *et al.* [20] carried out studies on concentration and velocity patterns observed in a horizontal rotating cylinder completely filled with a monodispersed suspension of non-Brownian positively buoyant particles and mapped out a phase diagram by varying the rotation rate and the solvent viscosity. One peculiar thing they noticed which was different from that of settling particles was that when centrifugal force dominates, the particles migrate toward the center. They also reported the formation of cone-like structures that occur just below the centrifugal limit.

Kalyankar *et al.* [20] proved experimentally that the differential centrifuging theory of Lee and Ladd [21] is not correct as stable band phase were seen for both positively buoyant as well as settling particles. Theoretically Lee and Ladd [21] predicted that settling particles experience an effective attraction leading to band formation, while buoyant particles experience an effective repulsion that disperses inhomogeneities in particle concentration.

Apart from the several monodispersed suspension experiments, a limited number of bidispersed suspension studies have been done. The bidispersity is mainly based on particle size. Structure formation in bidisperse sedimentaion is known to result from the difference in the settling velocities of the two species. Batchelor and Van Rensburg [22] have shown that in the Stokes flow regime for purely sedimenting suspension (without rotation) the structures result from instability of the statistically homogeneous dispersion to small concentration disturbances for certain combinations of values of the ratios of the sizes and densities of the two types of particles and their volume fractions. Kumar and Singh [23], performed experiments to characterize the axial segregation in bidispersed suspension of settling particles at various filling fractions and rotation speeds of the cylinder. The same mixture in the absence of carrier fluid did not show any segregation. In the case of particles suspended in water, it was observed that the rate of segregation increased with increase in filling fraction. From their work, they found out that the segregation pattern is dependent on the fill fraction and size of the particles. The number of bands decreased with increase in rotation rate.

Experiments with a bidispersed suspension of settling rod and spherical particles in a partially filled cylinder have revealed that banding occurred with each band having a

mixture of both types of particles [24]. In radial profile study of a bidispersed suspension by Jain *et al.* [25], segregation of particles occurred with heavier particles surrounded by the lighter ones. When the concentration of the heavier particles was increased, an increased segregation was observed, similar to the observations of Kumar and Singh [23].

Real everyday suspensions are characterized by a mixture of particles exhibiting differences in size, buoyancy, shape, etc., which would impart a complex interlink of interactions on the suspension behavior. This work is directed toward understanding the effect of having a mixture of particles of different buoyancy and shape in a bidispersed suspension on the particle segregation patterns and its comparison with the monodispersed suspensions.

II. EXPERIMENTAL METHOD

The particles used to make up the suspension include polystyrene spherical particles, glass beads and cylindrical nylon particles with densities of 1050 kgm^{-3}, 2450 kgm^{-3}, and 1150 kgm^{-3}, respectively. The mean diameters of the polystyrene and glass beads were 250 μm. The diameter and length of the cylindrical particles were 0.9 and 3.3 mm, respectively. The suspending fluid used was a mixture of aqueous glycerol and water prepared by taking proportionate amounts of the two liquids. Two solutions were prepared. The first solution made from 50 volume percent of aqueous glycerol had a measured density of 1139.32 kgm^{-3} and viscosity of 0.00476 Pas at 25°C. The other was a 35 volume percent aqueous glycerol having a measured density of 1098.72 kgm^{-3} and viscosity of 0.00233 Pas (at 25°C). Since the suspension constitutes different particle types, a mode of distinguishing them is required. The particles used in this work were coated with water-based acrylic dyes. The settling particles were coloured in red whereas the floating particles were coloured in blue.

In the experimental studies, a Pyrex glass cylinder of 1.28-cm inner diameter and length of 24.7 cm was used. This cylinder was connected by Teflon caps to a set of couplings rotating on ball bearings driven by a dc motor to rotate about the horozontal axis (as can be seen in the Fig. 1). The geometric aspect ratio (L/R) was approximately 38.6. The range of rotational speeds considered in our experiments was 7 to 127 rpm.

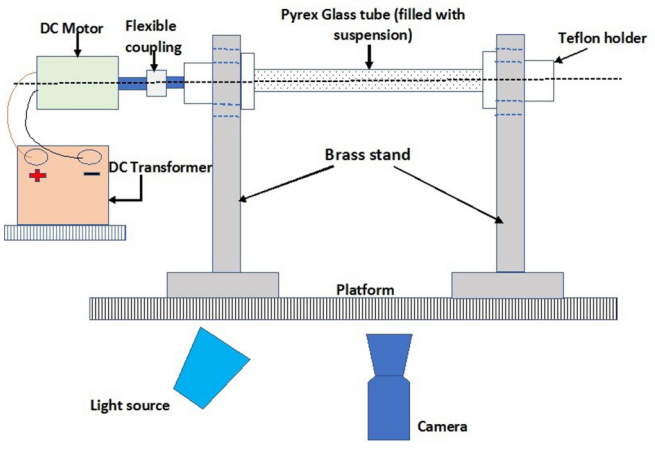

FIG. 1. Schematic diagram of the experimental setup.

To study the radial patterns of the bidispersed suspensions, another setup having a short cylinder of 2.39-cm diameter and 1.03-cm length in place of the long cylinder was used. The resulting geometric aspect ratio was approximately 0.86. These dimensions allowed us to carry out particle image velocimetry studies in the radial plane by following the spherical particles. This was possible because the length of the cylinder was much shorter compared to the diameter such that there was minimal defocussing of particles and negligible motion in the axial direction. In these studies, we analysed the influence of the buoyant particles on the pattern formation by the settling particles and the resulting trajectories of the settling particles. The images were captured with the help of two types of digital cameras. In the axial segregation studies, a CCD camera (Imperx B060) was used, while for the radial profile studies, a high-speed CMOS camera (Phantom Veo 640L) was utilised. Necessary arrangements were made to ensure horizontal levelling of the cylinder; the LED light was used to illuminate the flow field and for the rotational speed measurement, a noncontact tachometer was used.

The experimental work of axial segregation is described in two main parts. One involving a bidispersed particle system of spherical particles only, and the other consisting of a bidispersed suspension of cylindrical and spherical particles. In each of these cases, the monodispersed suspension is first analyzed and then the patterns are compared with the bidispersed system. The total particle volume fraction (ϕ) was maintained at 10%.

III. RESULTS AND DISCUSSION

The analysis and discussion of the results are set out in two parts with respect to the two bidispersed systems studied. The first involves a suspension of spherical settling and spherical floating particles while the second one is for a suspension of cylindrical settling and spherical floating particles. We provide parameters for the monodispersed suspensions in the form of dimensionless parameters. The particle Reynolds number, was given by $\mathrm{Re}_p = \frac{2aU_0\rho_f}{\eta}$, and Reynolds number based on angular speed, was computed using $\mathrm{Re}_d = \frac{\rho_f \omega R^2}{\eta}$, where ρ_s is the particle density, ρ_f is the fluid density, R is the internal radius of the cylinder and ω is the rotational speed. The Stokes velocity, is given by $U_0 = \frac{2}{9}\frac{a^2\Delta\rho g}{\eta}$, where a is the particle diameter, $\Delta\rho$ is the density difference between the particle and fluid, and η is the fluid viscosity. The Peclet number is given by $\mathrm{Pe}_p = \frac{U_0 a}{D_0}$, where D_0 is the Stokes-Einstein diffusion constant. Also, the Froude number was computed using the relation $\mathrm{Fr} = \frac{\omega^2 R}{g}$, where g is the acceleration due to gravity.

Case A: Bidispersed suspension of spherical settling and spherical buoyant particles

In the first set of experiments, we studied a suspension prepared from spherical glass beads (settling) and spherical polystyrene particles (floating). These particles were

TABLE I. Speed range of various phases of the monodispersed settling particle in a rotating cylinder. GB denotes the granular bed, F1 and F2 are the Fingering flow 1 and 2 respectively. LT is the low rotation rate transition while SB is the stable band phase.

Rotational speed (rpm)	Phase	Band no.	Band width (cm)	Re_d	Fr
7–15	GB	0	—	7.19–15.40	0.0004–0.0016
18–24	F1	0	—	18.48–24.64	0.0023–0.0041
29–74	F2	0	—	29.77–75.97	0.0061–0.0392
80–103	LT	14	1	82.13–105.75	0.0458–0.0759
108–127	SB	14	1.4	110.88–130.86	0.0834–0.1159

coated with red and blue acrylic dyes, respectively. The suspending fluid was 50-50 mixture (by volume percentage) of aqueous glycerol and water. For the glass beads, $\Delta\rho = 1310.68\,\mathrm{kgm}^{-3}$, while for the polystyrene beads $\Delta\rho = -89.32\,\mathrm{kgm}^{-3}$. The Stokes rising velocity (U_0) of the polystyrene beads was 0.0118 ms^{-1} and the Stokes settling velocity for the glass beads was 0.1724 ms^{-1}.

The monodispersed case was studied with reference to the phases reported by Matson *et al.* [3] for the setting particles and Kalyankar *et al.* [20] for the buoyant particles. The goal of this analysis was to obtain the patterns of the monodispersed suspensions at given rotational speeds for comparison with the bidispersed suspension at similar speeds. Several patterns comparable to those reported in the literature were seen and we summarize the observed particle behavior with corresponding speeds in Tables I and II. The particle Reynolds number (Re_p) was 10.862 for the settling particle suspension, while that for the buoyant particle suspension it was 0.3172. The corresponding Peclet numbers for the settling and buoyant particle suspensions were 2.87×10^{10} and 1.963×10^{9}, respectively. Considering the order of magnitude of the Peclet number for these suspensions, the Brownian motion effects can be neglected. As elaborated in the literature elsewhere [3,10,20,26], the patterns displayed a transition from a granular bed at very low speeds with the dominance of the gravitational forces to patterns characteristic of centrifugal force dominance. At the point when centrifugal force dominates, the settling particles are pushed to the wall while the buoyant particles traverse toward the central core. In between the two limits a variety of patterns are displayed. We notice that for the same speed, the band formation for the buoyant particle suspension initiates at relatively lower rotational speeds than the settling particle suspension.

TABLE II. Speed range of various phases of the monodispersed buoyant particle suspension. LT is the low rotation rate transition, HR is the homogeneous region, SB is stable bands, LD is the local structure drop-out, and DB is discontinuous banding.

Rotational speed (rpm)	Phase	Band no.	Band width (cm)	Re_d	Fr
7–10	LT	15	1.0	7.19–10.27	0.0004–0.0007
15–24	HR	0	—	15.4–24.64	0.0016–0.0041
34–63	SB	13	1.1	34.91–64.68	0.0084–0.0284
68–91	LD	12	0.6–1.2	69.81–93.43	0.0331–0.0591
97–127	DB	12	0.4–1.0	99.59–130.39	0.0668–0.1159

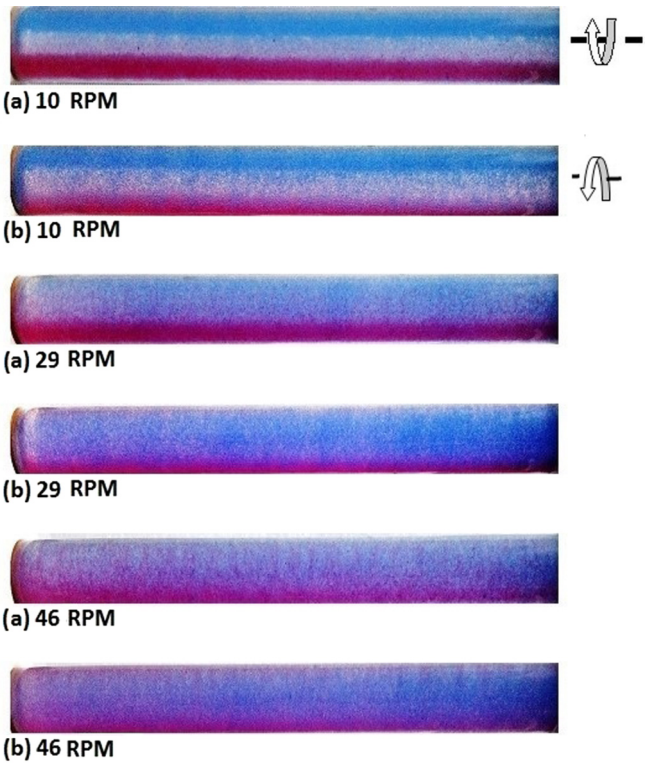

FIG. 2. Images showing the patterns (both front view **a** and back view **b**) of a bidispersed suspension of 5 percent volume fraction of spherical settling and an equivalent volume fraction of spherical floating particles rotating in anticlockwise direction at various speeds (up to 46 rpm). The blue (light gray) color represents the floating particles while the red (dark gray) color is for the settling particles.

The ease of band formation by the buoyant particles is likely due to the lower density difference and, hence, lower value of U_0 in comparison to the settling particles. Therefore, the particles are more easily dispelled from the bed. This would then lead to reduced resistance to the viscous forces. Since a given particle takes a longer time to return to the bed, thus it is more vulnerable to have its trajectory modified (this can also be deduced from the lower particle Reynolds number for the buoyant particles as compared to the settling particles).

The bidispersed suspension was made by mixing a 5% volume fraction of settling particles and an equivalent volume percentage of buoyant particles constituting a total particle volume fraction of 10%. It was noticed that for the various rotation speeds, the particles displayed a range of patterns which could be grouped into two; the first being the case where the two particle zones behave in a way that is almost independent of each other and the second where the patterns were a result of complementary influence of the two kinds of particles.

In Fig. 2, the images of the rotating bidispersed suspension for the rotational speeds ranging between 10 and 46 rpm are given. We would like to mention that the rotating cylinder was fixed on a rigid framework which was checked for horizontal alignment using a spirit level. It is possible that there was slight misalignment coupled with camera positioning and

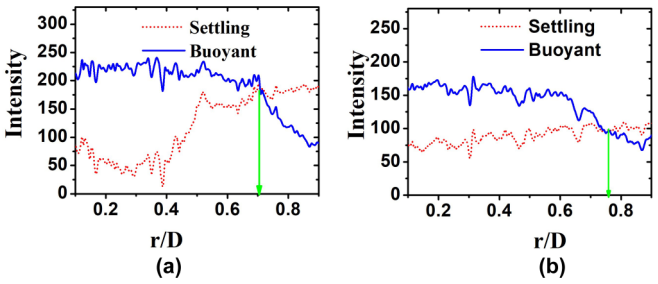

FIG. 3. The image intensity of blue and red particles plotted against the dimensionless distance (**r/D**) along a vertical line passing through the center of the cylinder. Here **r** is the distance along the diameter, measured from the top wall and **D** is the diameter of the cylinder. Plot **A** is for 7 rpm while **B** is for 24 rpm. The "blue solid line" represents the intensity variation for the floating particles while the "red dotted line" shows the intensity variation for settling particles.

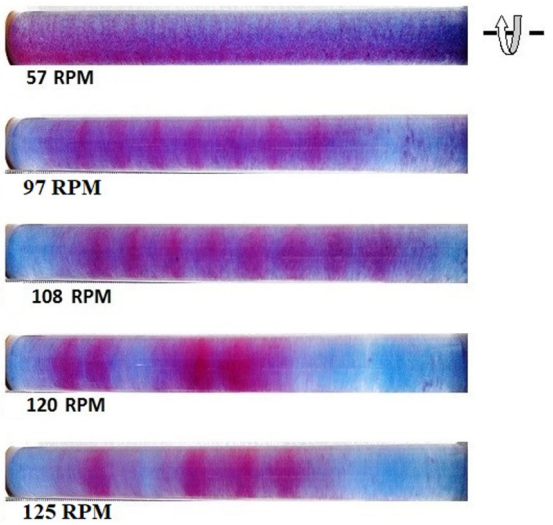

FIG. 4. Images showing the patterns for a bidispersed suspension of 5 percent volume fraction of spherical settling and an equivalent volume fraction of spherical floating particles rotating in anticlockwise direction at various speeds. The blue (light gray) color represents the floating particles while the red (dark gray) color is for the settling particles.

variation in the light intensity that seems to show up as particle layers not lying along the horizontal axis in some of the images. However, this has no bearing on the qualitative nature of the patterns. As a check, in some of the experiments we had reversed the direction of rotation and observed that the earlier configuration was recovered. Up to about 24 rpm, the two particle zones behave in a way that seems independent of each other. The buoyant particles prefer to stay on the falling side of the cylinder wall (being dragged downwards), while the settling particles show preference for the rising part of the cylinder wall, being dragged upwards. The buoyant particles display weak bands at 10 rpm which resembles LT phase reported by Kalyankar *et al.* [20] though not as prominent, probably due to the hindrance of the settling particle bed at the bottom of the cylinder.

The intensity of an image can be used to obtain qualitative information about the number density of particles. Figure 3 shows the intensity of the image along a vertical line drawn from top to bottom of the cylinder and passing through its axis. At the starting point of this profile, the intensity value for buoyant particles (blue color solid line) was initially greater indicating the proximity of the buoyant particle bed, but at the other extreme end of the vertical profile, the settling particles (red color dashed line) gave the greater intensity indicating the presence of the settling particle bed. Thus, in the graphs, the intersection of the buoyant particle intensity and the settling particle intensity represents the close approach to the vicinity of the boundary between the two particle zones. This is further elaborated in the radial profile studies in Sec. IV. The settling particle bed needs a higher rotation speed as compared to the buoyant particle bed so as to be dragged upwards, and as such, the greater portion of it stays at the bottom. The same is true with the rate of expulsion of particles from the settling bed, where the particles do not easily leave the bed as compared to the buoyant particles. The floating particle bed, however, easily moves downwards and as such, the front view reveals that the boundary between the two particle zones continuously descends toward the settling bed (Fig. 3). On the backside, the buoyant particle bed is continuously dragged downwards with increasing rotational speed while the settling particles are dragged on the rising side of the cylinder to approach the buoyant bed from above.

The patterns displayed at speeds greater than 24 rpm are characterized by the complementary influence of the two particle types. From the back view images in Fig. 2 for the speeds of 29 to 46 rpm, the settling particle bed was dragged up to the top wall at regular intervals and the buoyant particles occupied the positions between the two successive rings of settling particles. This became more prominent with increase in rotation speed.

Figure 4 gives the patterns observed for the rotating bidispersed suspension for speeds greater than 46 rpm. The patterns observed for 57 rpm are similar to those observed at 46 rpm. Considering the front view images for the speeds of 29 to 46 rpm (Fig. 2) and 57 rpm (Fig. 4), the settling particles are seen to trickle through the buoyant particles and there begins the appearance of a "finger-like" formation. These "fingers" became more prominent with increase in the rotation rate. In Fig. 5, the intensity variation along a profile line drawn at the center of the vertical axis across the axial direction is given for various rotational speeds.

At speeds greater than 57 rpm, the buoyant particles get fully engulfed by the settling particles, getting pushed toward the central core. At the speed of 97 rpm, patterns having a resemblance to the low rotation rate transition (LT) phase of the monodispersed suspension, characterised by asymmetric narrow bands and not clearly separated from each other appeared (see Fig. 5). Similarly, for 108 rpm, wider bands with close resemblance to the stable band (SB) phase were observed (see Fig. 5). These bands have a more symmetric distribution across the cylinder length, characterized by very low settling particle concentration in between them. For speeds greater than 108 rpm, the structure starts to breakdown, leading to discontinuous bands (DB), a phenomenon comparable

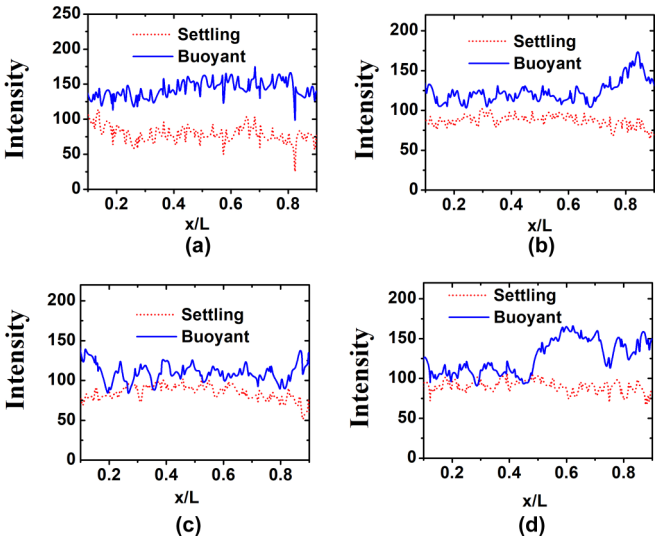

FIG. 5. The intensity of red (settling) and blue (buoyant) particles plotted against the dimensionless distance (**x/L**) along the cylinder axis. **L** is the total length of the cylinder (24.7 cm) and **x** is the distance along the axis measured from the left end of the cylinder. The plot **A** is for a rotational speed of 29 rpm and **B** is for 97 rpm. **C** and **D** are for speeds of 108 rpm and 114 rpm, respectively. The "blue solid line" represents the intensity variation for the floating particles while the "red dotted line" shows the intensity variation for settling particles.

to the behavior of the monodispersed suspension of settling particles.

Increasing the concentration of the settling particles above that of the buoyant particles was seen not to alter the kind of patterns observed apart from the increase in the number of bands and this can be observed in Fig. 6. The increase in bands observed when the concentration of the settling particles was increased, is attributed to increased segregation of the settling particles. The behavior of the bidispersed suspension

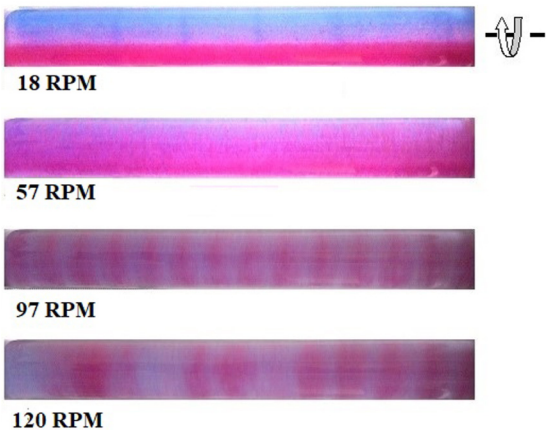

FIG. 6. Images showing the axial segregation patterns for a bidispersed suspension of 7.5 percent volume fraction of spherical settling and 2.5 volume fraction of spherical floating particles rotating in anticlockwise direction at various speeds. The blue (light gray) color represents the floating particles while the red (dark gray) color is for the settling particles.

TABLE III. The speed range for various phases of the monodispersed suspension of settling cylindrical shape particles. In the table, GB is the granular bed, F is the fingering flow, LT is the low rotation rate transition, SB is stable bands, LD is the local structure drop-out, and DB is discontinuous banding.

Rotational speed (rpm)	Phase	Band no.	Band width (cm)	Re_d
7	GB	0	—	14.16
10–29	F	0	—	20.23–58.66
34–40	LT	14	0.4–1.0	68.77–80.91
46–52	SB	13	1.1–1.3	93.04–105.18
63–74	LD	9–10	0.5–2	127.43–149.68
97–127	DB	8	1.0–4.4	196.20–256.87

as described above can be related to separate experiments we carried out with a higher concentration of monodispersed suspensions. In these experiments, we observed that bands started to form at lower rotational speeds when the suspension was more concentrated than the case when suspension concentration was lower. In their studies, Kumar and Singh [23] found out that increasing the concentration of the larger particles over the smaller particles resulted in increased segregation. The presence of the buoyant particles seems to lower the transition speeds at which various phases are observed for the monodispersed suspension. More elaborate particle arrangement and analysis of their interaction in the radial plane is given in Sec. IV.

Case B: Bidispersed suspension of cylindrical settling and spherical buoyant particles

In another set of experiments, the settling particles were cylindrical rods and the floating particles were spherical polystyrene beads coated with red and blue acrylic dyes, respectively. The suspending fluid used here was prepared by mixing 35% (by volume) aqueous glycerol and 65% (by volume) water. The density difference, $\Delta\rho$, between the cylindrical particles and suspending fluid was 51.28 kgm^{-3}, and for the polystyrene beads $\Delta\rho = -48.72\,\mathrm{kgm}^{-3}$. The behavior of a monodispersed suspension of cylindrical rods was first studied. This was then compared with the patterns observed with the bidispersed suspension.

Similar to the experiments described in case A, the total particle volume fraction was 10% with equal contribution from the spherical and cylindrical particles. The cylinder was rotated at various speeds and the particle behavior was recorded. In the Table III, we present a comparative categorization of the particle behavior observed with reference to the phases given by Matson *et al.* [3]. The Fig. 7 shows the resulting patterns of the monodispersed suspension for the various rotational speeds. A close up view of the particles is shown in the Fig. 8. The observed patterns have a resemblance to those for the spherical particles, showing similar transitions and this affirms the particle shape independence reported earlier by Seiden *et al.* [16] and Matson *et al.* [15]. At the start, when rotation is low, the particles form a bed close to the bottom of the cylinder, showing undulations at the top of the bed. As the rotational speed increased, the bed was dragged toward

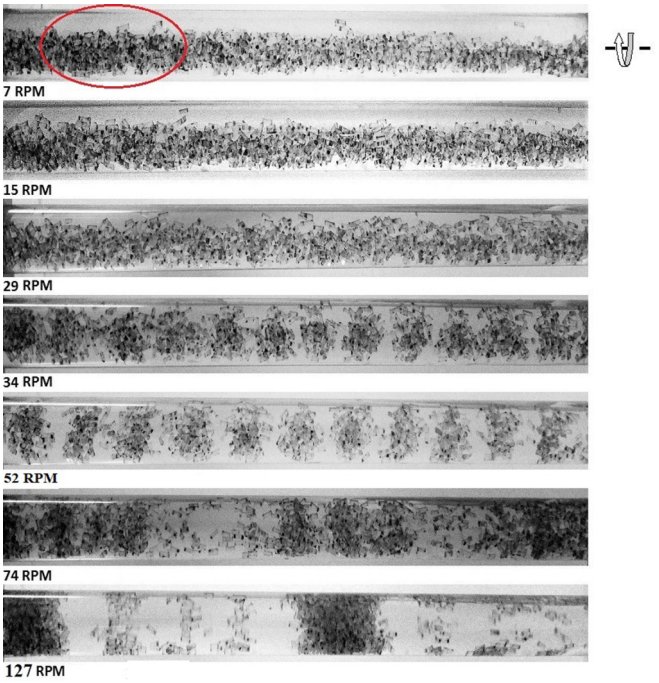

FIG. 7. Axial patterns of monodispersed suspension of cylindrical particles. The circled part is later zoomed in to view the particle arrangement at various speeds.

the top. The phase behavior was seen to be dominated by the gravitational force. As the bed was being dragged upwards, the particles were thrown out of the bed. During this processes these particles mostly aligned along the axis and occasionally changed their orientation when interaction with other particle occurred. When the speed was further increased, the intensity of particle collisions increased and the bed became disoriented, becoming more "porous." At the increased speeds, the particles dispersed throughout the suspending fluid and as such were vulnerable to the influence of the viscous drag and the centrifugal forces. The result was the lateral displacement and spinning of the particles which often lock into each other forming bands. The interesting behavior noticed was that the

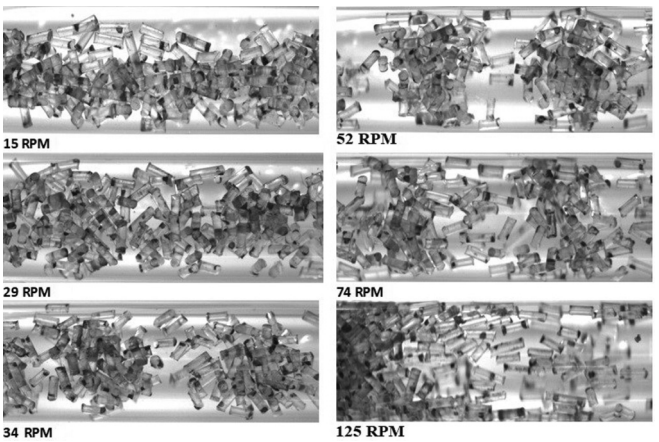

FIG. 8. Close up view of particle arrangement of the circled part in Fig. 7 for speeds of 15 to 125 rpm.

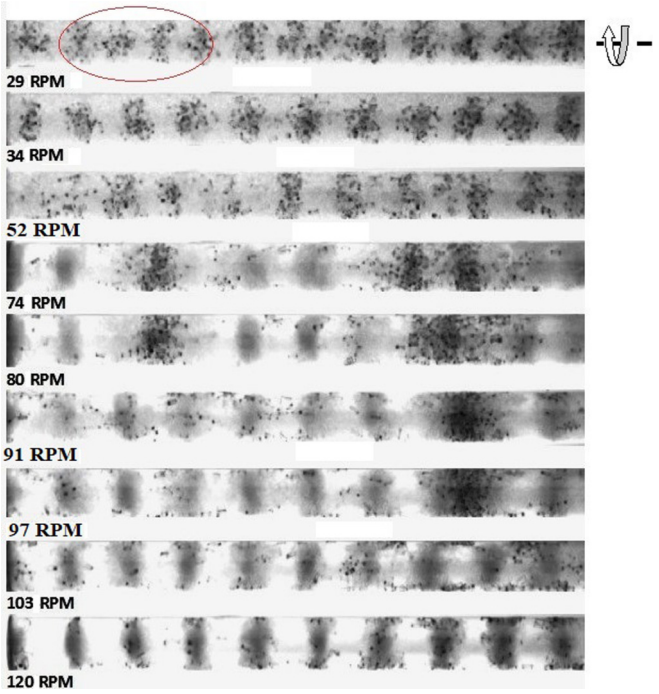

FIG. 9. Axial patterns of a bidispersed suspension of cylindrical settling and spherical floating particles in a horizontal cylinder rotating anticlockwise. The darker particles are cylindrical particles while the lighter ones are the spherical particles. In the next figure the circled portion is zoomed in to view particle arrangement at several rotational speeds.

cylindrical particles at the periphery always have a preference to lie along the lateral orientation of the cylinder, avoiding to spin in the direction of rotation. When they shifted from one band to the other, they did so without spinning across the lateral section of the cylinder.

The bidispersed suspension was made of 5% by volume of cylindrical particles and an equivalent volume fraction of spherical particles. In Fig. 9 the resulting axial patterns for various speeds are shown. Figure 10 gives a close view of particle distribution in the zone indicated in Fig. 9. The particle behavior can be categorized into two groups, i.e., one where the dominant patterns observed are those of the cylindrical particles and the other where the dominant patterns are coupled influence of the cylindrical and spherical particles. The former occurred at lower rotational speeds below 52 rpm while the latter happened for speeds above it.

It was observed that the cylindrical particles display patterns similar to those of the monodispersed suspension but the spherical particles did not show any band formation. This occurred up to the speed of 52 rpm, beyond which the bands of the spherical particles started to form. While the cylindrical particles traced their phases, the spherical particles were hindered from doing the same, most likely because of the orientation of the cylindrical particles which impose a "mixing" like effect on the surrounding spherical particles inhibiting them from forming bands. It was also noted that the observed patterns appear at lower speeds than they do for a monodispersed suspension of only the cylindrical particles. At 68 rpm, it was noticed that the buoyant particles were pushed

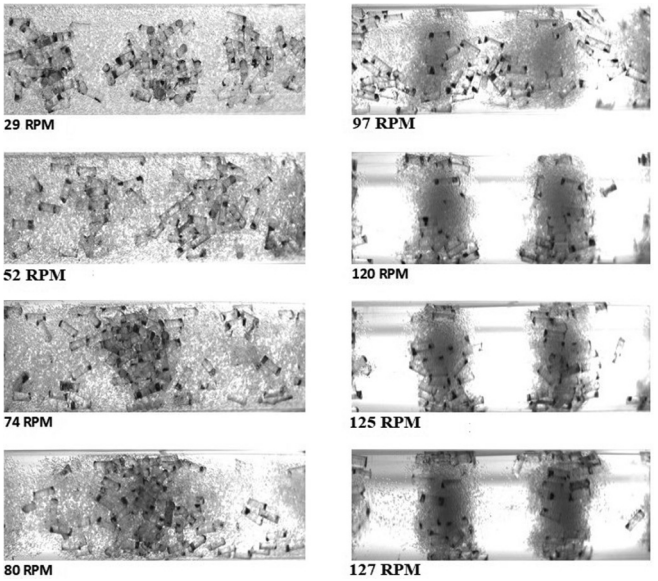

FIG. 10. Close view of the particle orientation of circled portion in Fig. 9 for the bidispersed suspension of cylindrical and spherical particles.

toward the inner core and as they did so, altered the patterns of the cylindrical particles. This influence was seen in the form of band formation of the buoyant particles at the core with the cylindrical particles at the cylinder walls. As the speed was increased, the number of bands increased. This progressed with more of the cylindrical particles being pushed to align parallel to the flow, at the cylinder wall. The alignment of the cylindrical particles along the wall translates into breakdown of the large discontinuous bands of the cylindrical particles. The band number of the spherical particles increases with increase in the rotational speed up to the speed of 120 rpm at which almost all the cylindrical particles are aligned parallel to flow along the cylinder wall and the corresponding widths of the bands are relatively similar across the cylinder length. Beyond this speed, no increase in band number was noted.

The density differences for this systems are comparable, and as such the particle displacement from their corresponding beds occur at almost the same rate. Much as this is so, the resulting patterns are dominated by the cylindrical particles because of the nature of their orientation (nonspherical and random with large degrees of freedom). The orientation of the cylindrical particles then creates what appears to be a kind of mixing effect on the surrounding buoyant spherical particles. Since by nature the settling particles traverse toward the cylinder walls in the centrifugal limit (and the reverse is true for buoyant particles) thus a core of buoyant particles is formed. As was seen in case A, the transition points of the phases of the dominant particle system (settling particles) occur at lower speeds than for the monodispersed suspension. This is attributed to the modification of the hydrodynamic interactions. Similar to the explanation given for case A, the settling and buoyant particles move in counter directions and this leads to alteration of the hydrodynamic interactions. At higher speeds, the cylindrical particles align themselves parallel to the axis of rotation at the wall, which then gives more liberty to the buoyant particles at the core. This provides space for the buoyant particles to re-organize into bands and this laterally displaces the cylindrical particles at the periphery (on the wall) around the formed stable bands. The detailed behavior of this system in the radial plane, indicating migration and orientation of the particles is discussed in Sec. IV.

IV. RADIAL PATTERNS

Radial profile visualization studies were carried out to gain insight into how the particles organize themselves in the radial plane. The high-speed CMOS camera (PhantomVeo 640L) was used to record the images at 800 frames per second with a resolution of 512 × 384 pixels. In these experiments a short cylinder was used, and the other components of the experimental setup remained the same as that of the axial segregation studies. Particle image velocimetry (PIV) studies were carried out by following the spherical particles. For the PIV analysis we used the Matlab toolbox, PIVLab version 1.42 [27]. The bidisperse suspensions studied were the same as those used in the axial segregation studies, i.e., one consisting of both spherical settling and spherical buoyant particles and the other consisting of cylindrical settling and spherical buoyant particles. The settling particles were coated with black acrylic dye while floating particles were not coated. The particle volume fractions for the bidisperse suspension of the spherical settling and spherical buoyant particles were 5% and 2.5%, respectively. In the second suspension, the particle volume fractions were 2.5 % for each of the constituent particles, i.e., cylindrical settling and spherical buoyant particles. The reduction in concentration as compared to that used in the axial segregation studies was intended to improve visualization. It was also proven that increase in concentration does not alter the patterns but only enhances segregation.

In their flow visualization studies, Perry *et al.* [28] showed that over very small time intervals, the streak lines, path lines and instantaneous streamlines were identical. Another aspect to consider is that when the flow is in steady state, the streamlines, streaklines and pathlines coincide since the Eulerian and Lagrangian descriptions become the same. In our experimental work, the time interval between the images captured is relatively small (1.25 ms). Hence, it is physically agreeable to make a direct comparison between PIV streamlines and the qualitative particle mean path lines.

In Fig. 11, the mean path lines and the corresponding streamlines and mean velocity magnitudes from the PIV analysis of the settling and buoyant particles is given. As seen from radial profiles of the bidisperse suspension of particles with the same shape (spherical), the buoyant particles descend toward the bottom of the cylinder, while the settling particles ascend toward the top of the cylinder. This is accelerated with an increase in the rotational speed. At high speeds, the buoyant particles disperse at the inner core and start reordering the settling particles. The reordering effect translates into quicker segregation of the settling particle phase.

In the speed range of 7 to 24 rpm, the boundary separating the settling particles from the buoyant particles at the bottom of the cylinder was nearly halfway from the center of the cylinder. As the speed increased, the settling bed reduced in size as it stretched extending upwards. The buoyant particles

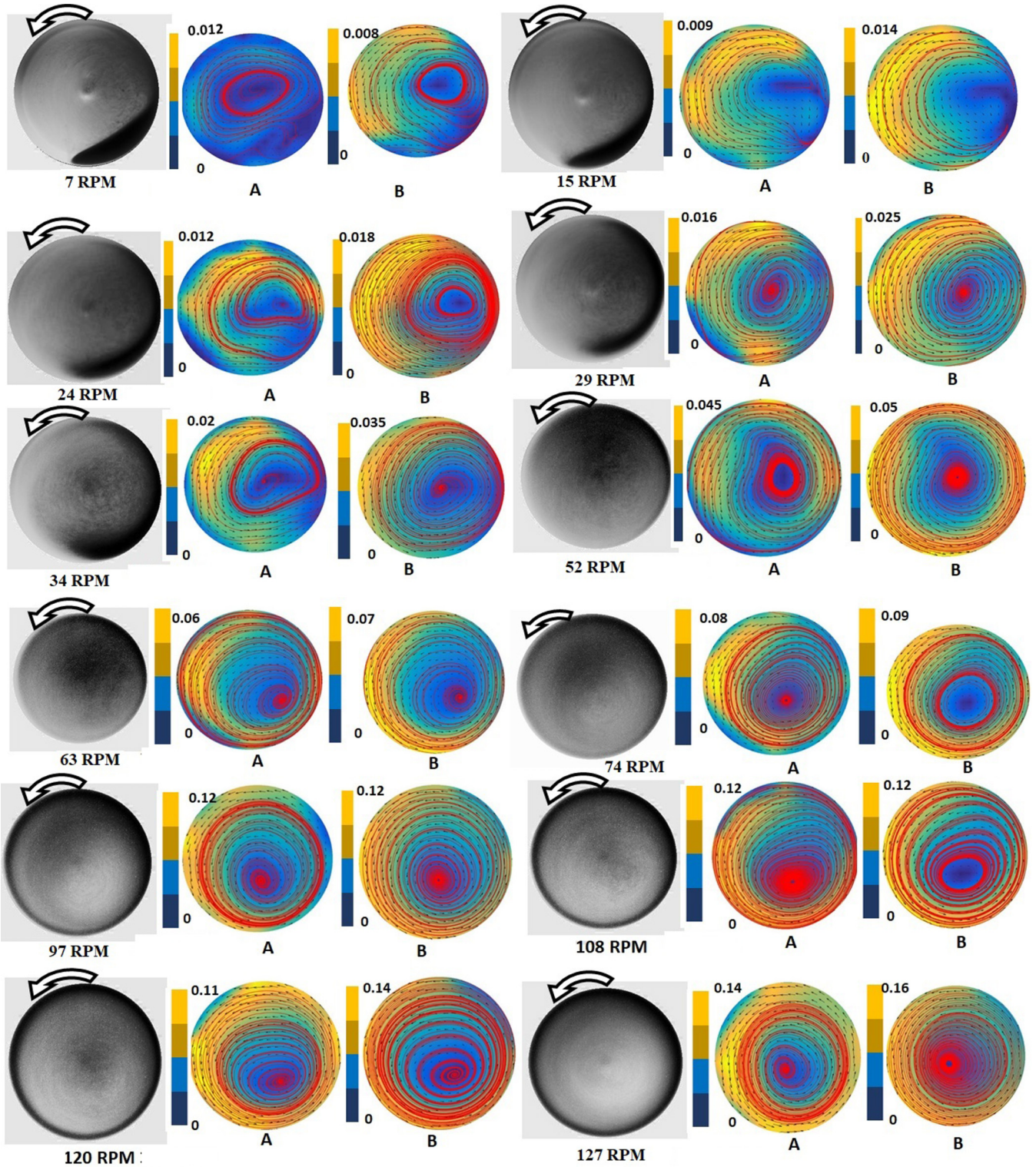

FIG. 11. Radial profiles of bidispersed suspension of spherical settling and spherical buoyant particles at various speeds. The gray-scale images shown in the left column are obtained from an overlay of 2000 frames at each speed. The resulting streamlines superimposed over the mean velocity vectors obtained from the PIV analysis of buoyant particles (column **A**) and the settling particles (column **B**) are also shown. The velocity magnitudes are in ms^{-1}. In the gray-scale images, the black or gray zones represent the settling particles while the white ones depict the buoyant particles.

did so in the opposite direction. This particle movement is related to the vertical particle boundary shifting (see Fig. 3). Particles stray away from both beds but their paths are dictated by the morphology of these beds. Initially, the small circulation of the buoyant particles is left-shifted while that of the settling particles is right-shifted. This left-shifted circulation is what is seen as weak transitional bands of buoyant particles in axial direction that was observed at 10 rpm and

shown in Fig. 6. The velocity magnitudes of the settling particles were initially lower than those of the buoyant particles but when the rotation speed was increased, the settling particles exhibited greater velocity magnitudes. This was so because more particles departed from the bed as it expanded.

In the case of rotational speeds between 29 and 34 rpm, as seen from Fig. 11, a tail of the buoyant particle bed extends into the settling particle bed at the bottom. The settling particle bed that had then reached the top of the cylinder did the same to the buoyant particle bed. The settling particles dispersed toward the left side and so did the buoyant particles toward the right. In either case, the particle beds limited how far and how wide the particle paths oriented themselves. At 52 rpm, interesting features were noted. The appearance of settling particles resembled a pendant liquid drop. This was an extension of settling particles whose bed was then at the top of the wall. The settling particles formed a dense core around which the buoyant particles circulated. The settling particles away from this core moved with a velocity close to that of the of the rotating cylinder walls. In the axial direction, this was seen as the "fingering" formations. In the range of 63 to 74 rpm, the settling particles detached from the bed at the top of the cylinder. The stretching of the particle bed along the circumference increased emanating from the top of the cylinder toward the bottom from either side. Reordering of the particles occurred such that spirals of particles leaning toward the right were formed with particles on the falling side of the cylinder having the greatest velocity magnitudes. This was so because the particle bed was right biased such that the particles far away from the bed moved freely without any hindrance. These patterns depict the characteristics exhibited by the lower transition state in the monodispersed suspensions. At 97 rpm, the settling particles had fully engulfed the buoyant particles. Here very distinct rings of the particles were noticed. The rings moved their axes near the center of the horizontal axis of the cylinder but the buoyant particles orbited in the confined inner zones. The settling particles spiralled across the entire domain and in relation to the axial segregation this corresponds to nondistinct bands as shown in Fig. 4. This observation is typical of the lower transitional state of monodispersed suspensions. The optimum velocity magnitudes were the same for both type of particles but the maximum velocity distribution for the buoyant particles was observed toward the left side. However, settling particle velocity was almost uniformly distributed and many had velocity magnitudes tending toward the maximum value. At 108 rpm, the optimum velocities of both particle types were equal and were also relatively uniformly distributed. Also, the rings formed by both spherical and cylindrical particles spanned the entire domain with a dense core of buoyant particles. This is seen as a characteristic reinforcement of the particles upon each other and is responsible for the distinct axial bands having clear boundaries.

For the speed of 120 rpm, the buoyant particles were seen to form circulation rings of particles confined to the core region with very few straying toward the wall. The buoyant particles were characterised by lower velocity magnitudes which were more uniformly distributed as compared to the settling particles. Settling particles formed rings stretching from the center to the walls of the cylinder. This feature is characteristic of the high transition phase in the monodisperse suspension. The maximum velocity lay to the left with a low-velocity zone at the core. This marked the starting of merging of the bands to produce large asymmetric bands in the axial direction.

At 127 rpm, more widely spaced rings of buoyant particles resulted but were confined within the core. As before, the velocity of these particles was more uniformly distributed near the walls though small in magnitude as compared to the settling particles. The settling particles formed two zones of rings of particles. One at the center and the other close to the wall. These rings were skewed toward the left. These features are typical of the behavior of discontinuous band phase of the monodispersed settling suspensions (please see Fig. 4).

In the case of the bidispersed suspension of spherical and cylindrical particles, the general motion in the radial plane was similar but significant qualitative difference in the patterns were observed (please see the Fig. 12). In the speed ranges of 7 to 15 rpm, the settling particles were dragged along the rising side of the cylinder wall, and progressively the bed got more porous and random. This was concurrently influenced by the infringing of the buoyant particles that arrive from the bottom. The buoyant particles orbited in the gap not inhabited by the settling particles and they extended their reach as the bed stretched. A noticeable difference at 15 rpm was uneven bed of the cylindrical particles, which is perhaps due to tumbling motion. Such contours were not observed in the previous case. At higher speed (24 to 29 rpm), the drag force was sufficient to lift the cylindrical particles away from the bed. In this process a group of cylindrical particles rotated together forming multiple circulation patterns. The center of these circulations was biased toward the rising side of the cylinder. With increase in speed the width of each ring increased and the center of these circulations was observed to shift toward the geometrical center of the cylinder. This kind of radial pattern appears to give rise the random interlocking patterns in the axial direction as depicted in the Fig. 9. With further increase in the rotation rate the stretch of the rings widened but its shape was somewhat deformed. At 34 rpm, the rings of the settling particles span the whole domain and had a broader width at the core. The buoyant particle rings were evenly distributed. It can be intuitively said that this particle arrangement yields the stable bands that was observed in the axial direction.

In the range of 46 to 52 rpm, more settling particles were pushed toward the wall increasing the buoyant particles concentration at the core. The number of rings formed by the cylindrical particles decreased with the rotation rate. As this happened, the buoyant particles core became denser. Such arrangement of particles is expected to produce discontinuous bands in the axial direction that was observed in Fig. 9. Between 63 and 80 rpm, the settling particles formed a thick ring close to the cylinder wall. The buoyant particles mostly occupied the inner regions. We observed that between 97 and 108 rpm, almost all the settling particles had aligned along the wall parallel to the axis as evidenced by the thin outer ring. This creates more room for the buoyant particles to freely rotate inside. This configuration is expected to form distinct and equally spaced uniform bands in the axial direction as seen in Fig. 7. The axial bands formed did not mix with each

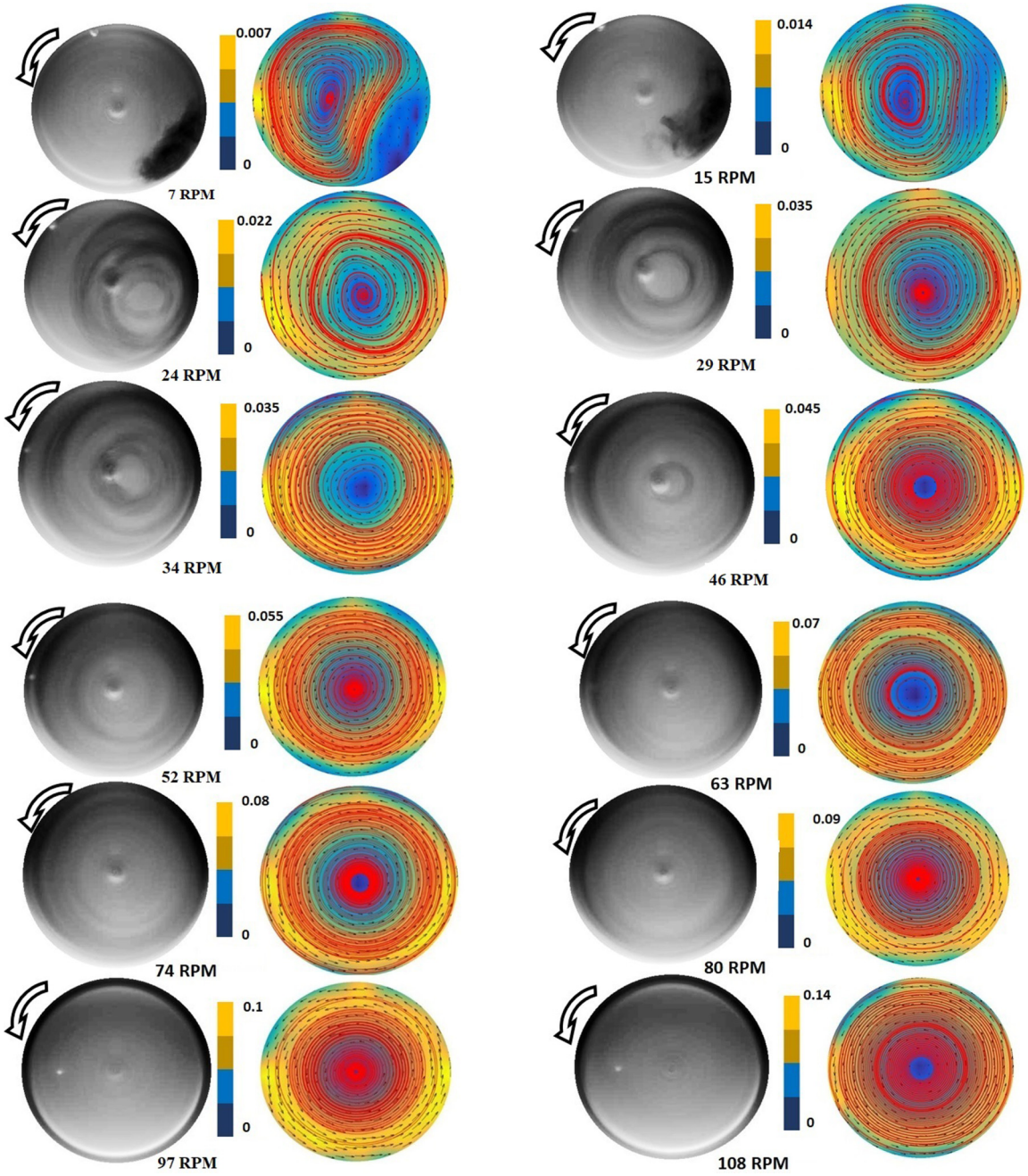

FIG. 12. Radial profile of bidispersed suspension of cylindrical settling and spherical buoyant particles. The gray-scale images in the left column were obtained from overlaying of 2000 frames taken for a given speed. In these images, the gray or black zones depict the settling particles while the white portions represent the buoyant particles. The streamlines superimposed over the velocity vectors (right column) obtained from the PIV analysis of the buoyant particles are also provided for each speed. The velocity magnitudes are in ms^{-1}.

other as was the case for partially filled cylinders [24] but rather made layers of settling particles at the periphery and buoyant particles at the core. This is similar to the observations by Jain *et al.* [25] for bidispersed suspension (based on the difference in relative densities) where a core of heavy particles and annular zone of lighter particles were formed.

In general, the buoyant particles caught up in the core of the settling particles enhances the particle-particle interactions modifying the hydrodynamic interactions. The frequent interactions make the system act like a concentrated suspension, as displayed by lower transition speeds for this phase. Considering these interactions influence the shear rate, the phenomena of shear-induced migration can also be suspected to come into play [29]. It is also interesting that in the work of Kozlov *et al.* [30] with two immiscible liquids in a rotating horizontal cylinder, the lighter liquid is pushed to the core and forms a column along the rotation axis while the heavy liquid forms an annular zone.

V. CONCLUSION

The bidispersed suspensions comprising a mixture of buoyant and settling particles showed the transition of the phases at lower speeds than the monodispersed suspensions of the respective settling particles. The phenomenon seems to show that the buoyant particles in a way enhance the local settling particle concentration lowering the transition speeds at which particular phases would occur. This is consistent with the results reported by Ramachandran and Leighton-JR [31] that increasing the particle volume fraction or concentration lowers the transition speed. Two distinct behaviors of the bidispersed suspension were observed: one is near independent motion of the buoyant and settling particles at lower rotational speeds and the second corresponds to the coupled influence of the these particles. The nonspherical nature of the cylindrical particles through their ability to rotate freely in the fluid imposes two significant influences, one at low rotation speeds and the other at very high rotation speeds. At low speeds, they bring about "mixing" of the spherical particles inhibiting their band formation, while at higher speeds due to the alignment along the cylinder wall, they enhance banding of the spherical particles. The overall lowering of the phase transition speeds and the resulting patterns can be attributed to the influence of the particle-particle interaction. This is seen through the difference in particle trajectories and alteration of the flow field in the fluid. This creates secondary flows that translate into the observed axial patterns.

[1] M. C. Roco, *Particulate Two-Phase Flow* (Butherworth-Heinemann, Boston, 1996).
[2] U. Schaflinger, *Flows of Particles in Suspensions* (Springer-Verlag, Wein, 1996).
[3] W. R. Matson, M. Kalyankar, B. J. Ackerson, and P. Tong, Phys. Rev. E **71**, 031401 (2005).
[4] P. T. Dbouk, Rheology of Concentrated Suspensions and Shear Induced Migration, Ph.D. thesis, Université De Nice-Sophia Anipolis, 2011.
[5] S. Mueller, E. Llewellin, and H. Mader, Proc. R. Soc. A **466**, 1201 (2010).
[6] H. Brenner, Annu. Rev. Fluid Mech. **2**, 137 (1970).
[7] M. Tirumkudulu, A. Tripathi, and A. Acrivos, Phys. Fluids **11**, 507 (1999).
[8] S. Lipson, J. Phys.: Condens. Matter **13**, 5001 (2001).
[9] S. Lipson and G. Seiden, Physica A **314**, 272 (2002).
[10] W. R. Matson, B. J. Ackerson, and P. Tong, Phys. Rev. E **67**, 050301 (2003).
[11] A. Breu, C. Kruelle, and I. Rehberg, Eur. Phys. J. E **13**, 189 (2004).
[12] R. F. Gans and Zupanski, Exp. Fluids **6**, 279 (1988).
[13] T. Krasnopol, G. V. Heijst, J. Voskamp, and S. Trigger, Int. Appl. Mech. **37**, 929 (2003).
[14] G. Seiden, M. Ungarish, and S. G. Lipson, Phys. Rev. E **76**, 026221 (2007).
[15] W. R. Matson, B. J. Ackerson, and P. Tong, J. Fluid Mech. **597**, 233 (2008).
[16] G. Seiden, S. G. Lipson, and J. Franklin, Phys. Rev. E **69**, 015301 (2004).
[17] G. Seiden, M. Ungarish, and S. G. Lipson, Phys. Rev. E **72**, 021407 (2005).
[18] J. Lee and A. J. C. Ladd, Phys. Rev. Lett. **89**, 104301 (2002).
[19] A. Breu and I. Rehberg, Europhys. Lett. **62**, 491 (2003).
[20] M. G. Kalyankar, W. R. Matson, P. Tong, and B. J. Ackerson, Phys. Fluids **20**, 083301 (2008).
[21] J. Lee and A. J. C. Ladd, Phys. Rev. Lett. **95**, 048001 (2005).
[22] G. K. Batchelor and R. W. J. Van Rensburg, J. Fluid Mech. **166**, 379 (1986).
[23] A. A. Kumar and A. Singh, Adv. Powder Technol. **21**, 641 (2010).
[24] G. Seiden and P. J. Thomas, Rev. Mod. Phys. **83**, 1323 (2011).
[25] A. Jain, A. Singh, and J. F. Brady, Radial segregation of settling suspension in a horizontally rotating cylinder, IUTAM symposium on Mobile particulate systems, Banglore (2012).
[26] W. R. Matson, B. J. Ackerson, and P. Tong, Solid State Commun. **139**, 605 (2006).
[27] W. Thielicke and E. J. Stamhuis, Journal of Open Research Software **2**, e30 (2014).
[28] A. E. Perry, M. S. Chong, and T. T. Lim, J. Fluid Mech. **116**, 77 (1982).
[29] D. Leighton and A. Acrivos, J. Fluid Mech. **181**, 415 (1987).
[30] N. V. Kozlov, A. N. Kozlova, and D. A. Shuvalova, Phys. Fluids **28**, 112102 (2016).
[31] A. Ramachandran and D. T. Leighton Jr., J. Fluid Mech. **603**, 207 (2008).